SDG Indicator 6.6.1. Change in the extent of water-related ecosystems over time

Methodology for the use of satellite-based Earth observations datasets and respective tools for country level reporting

Prepared by: Raha Hakimdavar, Mark Carroll, Sandeep Chittimalli, Lola Fatoyinbo, Matthew Hancher, Matthew Hansen, Alfred Hubbard, Margaret Hurwitz, Argyro Kavvada, David Lagomasino, Nima Pahlevan, Amy Pickens, Frederick Policelli, Peter Potapov, Brandon Smith, Sushel Unninayar, Danielle Wood

October 2017

Table of Contents

List of Figures

List of Tables

1. Introduction

Global monitoring of Sustainable Development Goal (SDG) 6 – ensure availability and sustainable management of water and sanitation for all – was initiated in early 2017 following development, testing, and evaluation of methodologies for monitoring the associated indicators. Target 6.6 of SDG 6 calls for the protection and restoration of water-related ecosystems, including mountains, forests, wetlands, rivers, aquifers and lakes. The first indicator of this target, Indicator 6.6.1, tracks changes over time in the extent of water-related ecosystems. UN Environment is the custodian agency for this indicator and has developed a step-by-step methodology that explains how to monitor change in the extent of water-related ecosystems over time, including definitions, computational steps, and recommendations on spatial and temporal resolutions. Custodian agencies are charged with producing methodologies for collecting data from national data sources and tracking progress, as well as contributing towards statistical capacity building, among other key activities. While analysis of ground-based, survey data and in-situ measurements serves as an important part of the reporting process, there is potential for countries to utilize satellite-based Earth observations (EO) to meet some of the reporting requirements of Indicator 6.6.1, pertaining to both spatial extent and quality of open waterbodies and wetlands.

In collaboration with the Group on Earth Observations (GEO) and space agencies such as NASA, ESA, and JRC, UN Environment has identified a series of activities that focus on the use of EO to support the monitoring and data collection process for Indicator 6.6.1. These pilot efforts do not intend to replace the country-owned process of SDG data collection and submission; rather, they intend to explore the applicability of EO data to complement country-generated data.

This document provides an overview of the datasets and methodology used by a NASA-University of Maryland team to demonstrate the potential for EO data to be used for monitoring the SDG Indicator 6.6.1. For the purpose of this document, EO data is defined as data that is gathered via remote sensing technologies. The current assessment focuses on the ecosystem categories of vegetated wetlands (coastal mangroves only) and inland waters (rivers and estuaries, lakes and reservoirs). Two of the three principle water ecosystem sub-indicators, as defined by the UN Water publication “Integrated Monitoring Guide for SDG 6”, are measured: the spatial extent of water-related ecosystems, and the quality of water within these ecosystems. It is noted that a fourth sub-indicator, to measure the state or health of ecosystems, is also listed as a sub-indicator for Indicator 6.6.1, however it does not form part of the aggregated 6.6.1 index – rather, this is kept for national level reporting and to assist w/ restoration activities Datasets used, methodologies and preliminary results for the following aspects of the indicator are provided in this report:

1. Spatial extent for open waterbodies,
2. Total Suspended Solids and Chlorophyll for inland waterbodies,
3. Spatial extent for coastal mangroves.

Each section provides an overview of the datasets and tools used – including spatial resolution, required software, data output format and relevant publications – as well as the methodology used and results in terms of country-level statistics, where applicable. The methodologies shared in this report are not a comprehensive summary of the steps required to extract relevant information from raw remote sensing data, but rather an overview of the steps that should be taken to analyze existing pre-processed datasets stemming from remote sensing, in order to meet the goals for baseline SDG reporting.

2. Overview of the pilot study

The goal of the pilot study is to extract information relevant to meeting the reporting requirements of SDG Indicator 6.6.1 from EO data for a select group of pilot countries, utilizing openly available, free of charge datasets and tools (see Table 1). In this regard, the study serves as a proof of concept for the use of EO data in SDG reporting. In its custodian agency role, UN Environment will subsequently aim to efficiently distribute the successful methods and datasets to countries to support their data-driven decision-making regarding this indicator.

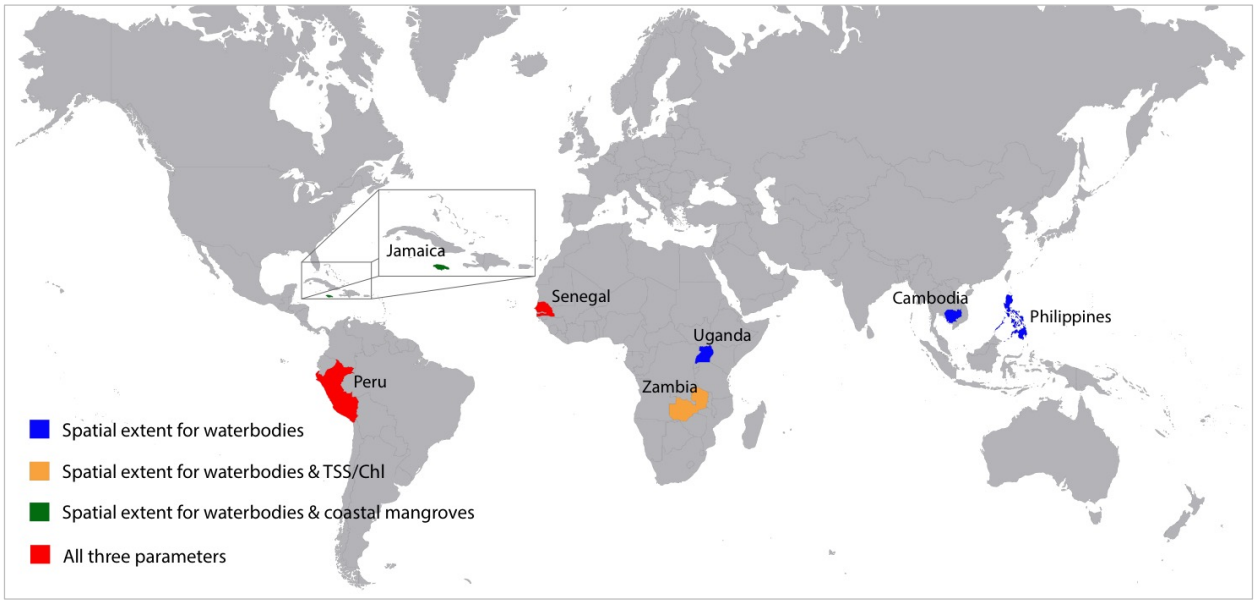

Figure 1 – Map of the countries considered in this pilot effort, with the parameters/sub-indicators investigated.

As shown in Figure 1, for the extent of open waterbodies, the pilot countries included Cambodia, Jamaica, Peru, Philippines, Senegal, Uganda and Zambia. A proof of concept for the extraction of the water quality indicators of Total Suspended Solids and Chlorophyll was also provided for select large open waterbodies in the countries of Peru, Senegal and Zambia. Pilot countries for the spatial extent of coastal mangroves included Jamaica, Peru and Senegal. It is important to note that the pilot countries ranged in size and spatial complexity in terms of landscape variability, thus covering a range of capabilities for the application of the EO data. Where possible, country-level statistics were extracted, reporting on the area of water and coastal mangrove extent, as would be required by all countries for their SDG reporting. It is noted that this document serves as a general guide for the potential use of EO data in meeting some of the reporting requirements for the SDG Indicator 6.6.1 and is in no way providing official country baseline values for the indicator. The derived datasets will ultimately be published on an online database, and in the meantime, can be provided to interested parties upon request. More information and updates are available on http://eo4sdg.org/earthobservations-for-sdg6monitoring/.

Water Ecosystem Measured	Sub-indicators Measured	Datasets	Spatial Resolution (m)
Open water	Spatial extent	MOD44W C6.1*	250
Open water	Spatial extent	Landsat-5, 7, and 8*†	30
Lakes & reservoir	TSS and Chlorophyll	Landsat-8*† and Sentinel-2A‡	20-30
Wetlands (coastal mangroves)	Spatial extent	Landsat 8 OLI*†, Sentinel-1C‡, SRTM*	30

*National Aeronautics and Space Administration (NASA) †US Geological Survey (USGS) ‡European Space Agency (ESA)

Table 1 - Summary of the components measured and datasets used for the pilot study. Note: Copernicus Sentinel data is processed by the European Space Agency, and was retrieved in 2017 for this effort.

3. Mapping and quantifying the spatial extent of open waterbodies (using MOD44W C6.1)

3.1. Overview

Water Ecosystem(s) Measured: Open water

Sub-indicator(s) Measured: Spatial extent

Dataset(s): MOD44W C6.0

Data Source(s):
This dataset is a collection of global, annual water maps in raster format. These datasets were created by applying a water identification algorithm to data from the MODerate Spatial Resolution Imaging Spectrometer (MODIS), on board the Terra satellite. The data shows normal surface water extent for each year. The data is available for every year from 2000 through 2015, and for every major land mass, excluding Antarctica. Figure 2 shows the MOD44W C6.0 dataset for Lake Bangweulu, Zambia, in the year 2014.

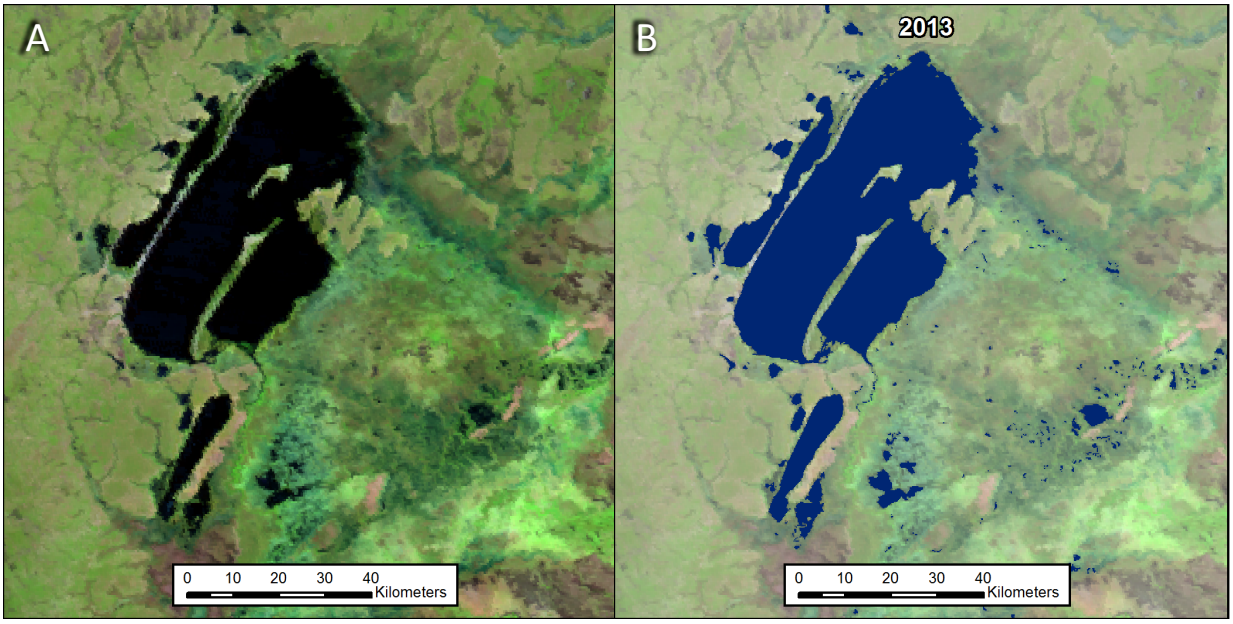

Figure 2 - A) False color composite (6-2-1) MODIS surface reflectance image (MOD09A11) of several lakes, the largest of which is Lake Bangweulu, and associated swamps in Zambia. Imagery is an 8-day composite collected from a period beginning on 7/12/13. B) The annual water dataset, MOD44W C6.0 (Carroll et al., 2017), overlain in blue, showing measured spatial extent of open water for the year 2013. [1]Vermote, E., et al., 2015, MOD09A1: MODIS/Terra Surface Reflectance 8-Day L3 Global 500m SIN. Version 6. NASA EOSDIS Land Processes DAAC, USGS Earth Resources Observation and Science (EROS) Center, Sioux Falls, South Dakota (https://lpdaac.usgs.gov), accessed 06 23, 2017, at http://dx.doi.org/10.5067/MODIS/MOD09A1.006

Spatial Resolution: 250 m

Required Software: ArcGIS, QGIS, or other desktop GIS application

Output Format(s): Geo-referenced raster dataset (e.g. GeoTIFF)

Relevant Publications:
Publication of the data is still in progress, but it can be cited as:

- Carroll, M.L., DiMiceli, C.M., Hubbard, A.B., Wooten, M.R., Sohlberg, R.A., Townshend, J.R.G. (2017). Global Raster Water Mask at 250 meter Spatial Resolution (MOD44W) Collection 6.0.

A user guide will be released at the same time as this data. Also, the algorithm used to create this data was previously described in the following paper:

- Carroll, M.L., Townshend, J.R., DiMiceli, C.M., Noojipady, P., & Sohlberg, R.A. (2009). A new global raster water mask at 250 m resolution. International Journal of Digital Earth, 2, 291-308

3.2. Methodology

To measure the area of water in a given area at a given time, the GeoTIFF rasters associated with this dataset are needed, a polygon shapefile covering the area of interest, and a computer running a desktop GIS application. Obtaining the latter two items is beyond the scope of this guide. This guide will recommend specific procedures based on the assumption that users are working in ArcGIS, but analogous operations are most likely available in other GIS applications. As for the open water dataset itself, MOD44W C6.0 will ultimately be published on an online database, and this guide will be updated with the relevant links at that time. For now, the necessary data files will be made available by NASA to interested parties.

Each year of data has a separate set of raster files. The following procedure applies to one year of data, and it should be repeated when analyzing multiple years. Including multiple years is recommended in most cases, because water extent can change considerably from year to year.

The GeoTIFF files that make up MOD44W C6.0 are organized according to the MODIS tiling system (https://modis-land.gsfc.nasa.gov/MODLAND_grid.html), which divides the globe into a grid of square tiles. The first step is to determine which tiles overlap the area of interest and, if there is more than one of them, mosaicking (i.e. combining) those into one dataset. An image of the MODIS tiling system is provided in the above hyperlink, which can help determine which tiles are necessary. Many tools exist for mosaicking images. To do so in ArcMap, one of two tools/operations can be used: “Create Mosaic Dataset” and “Add Raster to Mosaic Dataset” tools, or the “Mosaic to New Raster tool.”

Once the raster or rasters of interest are obtained, the next step is to use the shapefile demarking the area of interest to mask out areas that are not inside this area. This shapefile could be the boundary of a country, the boundary of a sub-national administrative unit, a polygon enclosing a specific waterbody, or any other polygon shapefile. If the polygon is intended to enclose a specific waterbody, it is recommended that the polygon be created to leave a significant buffer area around the waterbody in question. Many waterbodies fluctuate significantly over the course of time, and a shape drawn based on one image or map may not contain the entire waterbody in a different image. Regardless of the source of the polygon shapefile, the procedure to use it with the water data remains the same. Use a tool, such as Extract by Mask in ArcGIS, to extract the portion of the water raster that intersects this polygon into a new raster file. This new raster should only contain data where it overlaps the polygon of interest.

Finally, to get the area of water for this region, open the attribute table for the new raster file that was created above. In ArcMap, this can be accomplished by right-clicking the layer in the Table of Contents and selecting “Open Attribute Table.” In this table, the count of pixels for each raster value is displayed. Water is signified by a “1” in this dataset, and so the count of pixels that have a value of “1” is of interest.

This count can be converted to area by multiplying by the area of a pixel. For this dataset, that area is $(231.65635\ m)^2$, or 53664 m^2, or 0.05366 km^2. The result of this multiplication is the area of surface water within the polygon of interest, as measured in the MOD44W C6.0 dataset.

3.3. Results

Table 2 – Spatial extent of open waterbodies for the seven pilot countries, extracted using the MOD44W C6.0 dataset, as described in the above methodology. The reported areas represent the spatial extent of national open waterbodies for different years.

Country	2011 [km^2]	2012 [km^2]	2013 [km^2]	2014 [km^2]	2015 [km^2]
Cambodia	9465.16	5458.50	7507.36	6538.18	4645.21
Jamaica	29.41	27.48	29.14	29.41	29.68
Peru	13136.25	13681.16	13476.70	13005.85	13163.19
Philippines	6410.03	6338.82	6393.55	6366.45	6415.02
Senegal	1495.42	1478.30	1509.53	1460.16	1399.95
Uganda	36570.97	36610.79	36634.72	36599.68	36659.67
Zambia	12404.53	12443.71	12312.12	13097.40	12057.16

Source of Administrative boundaries: The Global Administrative Unit Layers (GAUL) dataset, implemented by FAO within the CountrySTAT and Agricultural Market Information System (AMIS) projects.

3.4 Contributors

Alfred Hubbard, Mark Carroll, and Frederick Policelli all contributed to the preparation of materials for NASA's support of this SDG initiative. For the authors involved in the creation of MOD44W C6.0, please see the above citation.

4. Mapping and quantifying the spatial extent of open waterbodies (using Landsat)

4.1. Overview

Water Ecosystem(s) Measured: Open water

Sub-indicator(s) Measured: Spatial extent

Dataset(s): Landsat 5, 7, 8 archive

Data Source(s): > Not currently hosted anywhere

Spatial Resolution: 30 m

Required Software: Any geographic software, e.g. QGIS, PCI, ArcMap, ERDAS, etc.

Output Format(s): GeoTiff

Relevant Publications:
Quantifying global monthly water dynamics 1999-2017 *(In Preparation)* Pickens, A.H., Hansen, M.C., Hancher, M.D., Potapov, P.

4.2. Methodology

The GLAD water dynamics layers were created through an automated process mining the entire 1999-2015 Landsat 5, 7, and 8 archive. A quality assessment (QA) model, which was developed locally, was applied to every single scene with the computing power of Google Earth Engine.

After conversion to top of atmosphere (TOA) reflectance, each scene was classified into land, water, cloud, shadow, haze, and snow and ice. This was done via five heirachical sets of seven bagged classification trees utilizing all the image bands, ratios of each pair of bands, and 3x3 pixel spatial averages of all bands and ratios. Elevation and derived slope and aspect data were used as additional metrics. Elevation was taken from Shuttle Radar Topography Mission (SRTM) elevation for everywhere south of 60°N, and Global Multi-resolution Terrain Elevation Data 2010 (GMTED2010) for everywhere north of 60°N. These classification trees were built from a training set of 120-160 fully classified scenes per sensor.

All of the land and water observations of a given pixel are summed per month per year. From these layers the data is further aggregated into seasonal and annual water presence frequency, measured by the percent of clear observations flagged as water. An interannual trend model has been applied per season and for all twelve months together that is able to capture the broad dynamics of surface water extent through the entire time period (Figure 1). All layers have 0.00025° resolution, which is equivalent to 28m at the equator.

For the UNEP baseline of 2013-2015, if more than 50% of the observations without cloud, haze, shadow, or snow from those years are labelled water, then the pixel is labelled water for the baseline map. Pixels that only no land or water observations for all three years are labelled no data. The resulting map represents permanent and semi-permanent inland water. The area of all water pixels is summed to find the spatial extent of open waterbodies (Table 1).

4.3. Results

Table 3 – Spatial extent of open waterbodies for the seven pilot countries, extracted using Landsat data, as described in the above methodology. The spatial extent was calculated by summing the area of all the persistent water pixels in the baseline 2013-2015 layer within each country boundary. The initial data volume represents the terabytes (TB) of Landsat data that was processed.

Country	Assessment period	Spatial extent of national open waterbodies (km^2)	Initial Data Volume (TB)
Cambodia	2013-2015	6469	1.81
Jamaica	2013-2015	38	0.56
Peru	2013-2015	18210	6.98
Philippines	2013-2015	7002	3.93
Senegal	2013-2015	2012	2.16

Uganda	2013-2015	36257	2.43
Zambia	2013-2015	13734	5.54

Source of Administrative boundaries: The Global Administrative Unit Layers (GAUL) dataset, implemented by FAO within the CountrySTAT and Agricultural Market Information System (AMIS) projects.

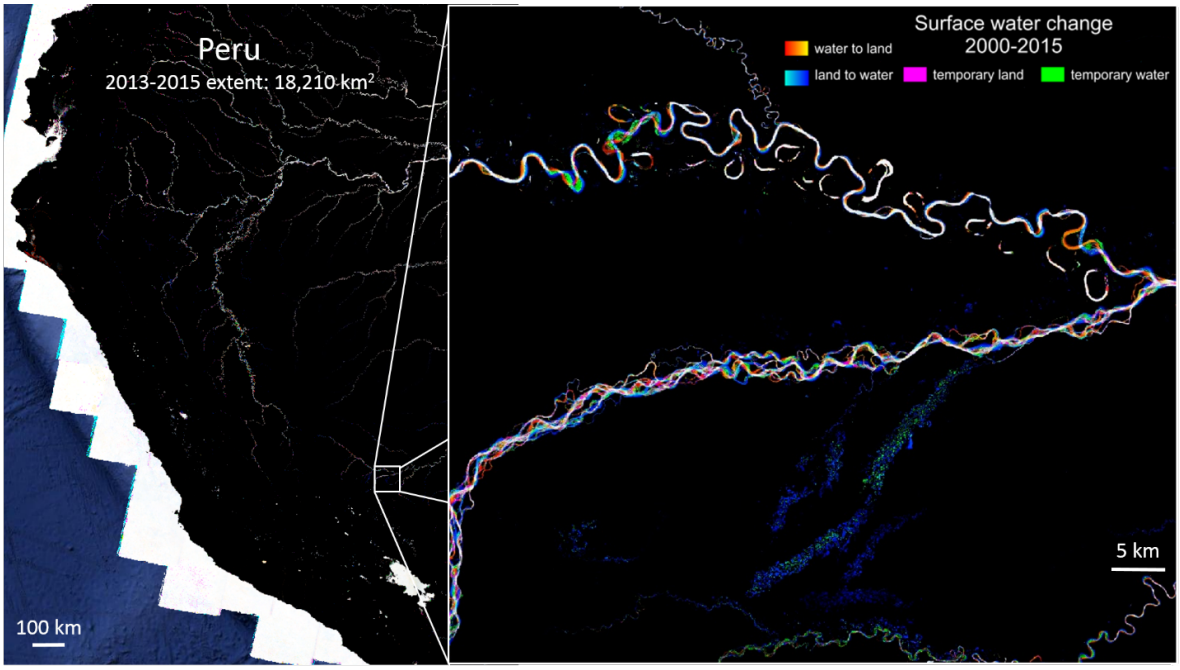

Figure 3 – Interannual surface water dynamics 1999-2015 for all 12 months in Peru. The zoom window on the right shows the meandering rivers as well as new ponds for mining operations in Madre de Dios.

4.4. Contributors

Amy Pickens, Matthew Hansen, Matthew Hancher, Peter Potapov

5. Mapping and quantifying concentrations of Total Suspended Solids and Chlorophyll for inland waterbodies

5.1. Overview

Water Ecosystem(s) Measured: Inland waters

Sub-indicator(s) Measured: Water quality (Concentration of Total Suspended Solids and Chlorophyll)

Dataset(s): Landsat-8 and Sentinel-2A

Data Source(s): https://earthexplorer.usgs.gov ; https://scihub.copernicus.eu/dhus/

Spatial Resolution: Landsat-8: 30m; Sentinel-2A: All bands resampled to 20m

Required Software: https://seadas.gsfc.nasa.gov

Output Format(s): netcdf

Relevant Publications:

Gordon, H.R., & Wang, M. (1994). Retrieval of water-leaving radiance and aerosol optical thickness over the oceans with SeaWiFS: a preliminary algorithm. Appl. Opt., 33, 443-45

Nechad, B., Ruddick, K., & Park, Y. (2010). Calibration and validation of a generic multisensor algorithm for mapping of total suspended matter in turbid waters. Remote Sensing of Environment, 114, 854-866

O'Reilly, J.E., Maritorena, S., Siegel, D.A., O'Brien, M.C., Toole, D., Mitchell, B.G., Kahru, M., Chavez, F.P., Strutton, P., & Cota, G.F. (2000). Ocean color chlorophyll a algorithms for SeaWiFS, OC2, and OC4: Version 4. SeaWiFS postlaunch calibration and validation analyses, part, 3, 9-23

Pahlevan, N., Sarkar, S., Franz, B.A., Balasubramanian, S.V., & He, J. (2017a). Sentinel-2 MultiSpectral Instrument (MSI) data processing for aquatic science applications: Demonstrations and validations. Remote Sensing of Environment, 201, 47-56

Pahlevan, N., Schott, J.R., Franz, B.A., Zibordi, G., Markham, B., Bailey, S., Schaaf, C.B., Ondrusek, M., Greb, S., & Strait, C.M. (2017b). Landsat 8 remote sensing reflectance (R rs) products: Evaluations, intercomparisons, and enhancements. Remote Sensing of Environment, 190, 289-301

Tyler, A.N., Hunter, P.D., Spyrakos, E., Groom, S., Constantinescu, A.M., & Kitchen, J. (2016). Developments in Earth observation for the assessment and monitoring of inland, transitional, coastal and shelf-sea waters. Science of the Total Environment, 572, 1307-1321

5.2. Methodology

With the high-frequency revisit time of combined Landsat (a NASA-USGS mission) and Sentinel-2 (an ESA mission) satellites, it is now possible to utilize the respective satellite products for regular monitoring of aquatic systems in nearshore coastal and inland waters (Tyler et al. 2016). EO data can only provide information on concentrations of in-water materials that affect the color of water. These materials include chlorophyll-a (Chl), which is the primary pigment in phytoplankton (the primary source of food for organisms), and the total suspended solids (TSS). The concentrations of Chl and TSS can be used as proxies to infer other important parameters like oxygen level, nutrients, or chemicals. For instance, high TSS in a water body can often mean higher concentrations of bacteria, nutrients, pesticides, and metals in the water. Chl and TSS are both listed as SDG indicators require monitoring in lakes and riverine systems.

In this study, we use widely used empirical algorithms to produce concentrations of TSS and Chl in different lake systems in Zambia, Peru, and Senegal. While the TSS algorithm uses information in the red spectral bands (Nechad et al. 2010), the Chl retrieval is based upon the heritage ocean color algorithm (O'Reilly et al. 2000), which uses band ratio of green and blue bands. The Landsat-8 and Sentinel-2A images are processed using NASA's SeaWiFS Data Analysis System (SeaDAS) (https://seadas.gsfc.nasa.gov). The system conducts atmospheric correction (Gordon and Wang 1994) and then applies atmospherically corrected in-water reflectance to derive TSS and Chl.

We chose five different aquatic systems, namely Lake Bangweulu in Zambia, Lake Titicaca and Lake Chinchayqucha in Peru, Casamance River and Lake Guiers in Senegal. We chose arbitrary locations within each system to plot the relative changes in Chl and TSS over time since 2013. The data extracted over selected areas, i.e., 6×6- and 9×9-element windows from OLI and MSI products, respectively. In this analysis, the relative variations in OLI- and MSI-derived products are of interest and the precision/accuracy in retrievals of TSS or Chl is beyond the scope of this research.

Figure 4 - Five different lakes (highlighted in with red boxes) in Zambia, Peru, and Senegal studied here.

5.3. Results

The time-series begin two months after Landsat-8 launch, i.e., Feb 13th 2013, and data points show retrievals when valid OLI or MSI data products are available, i.e., cloud-less conditions. In the following plots, TSS and Chl are provided in units of gm-3 and mgm-3. One example of the spatial distributions of TSS and Chl is shown (left) for each site. The dynamics of water quality in different bodies of waters is inferred from the temporal plots. In particular, it is noted that satellite data products can detect anomalies in water quality conditions if processed via appropriate tools. The time-series plots are shown for an area marked with a cross in the map to the left.

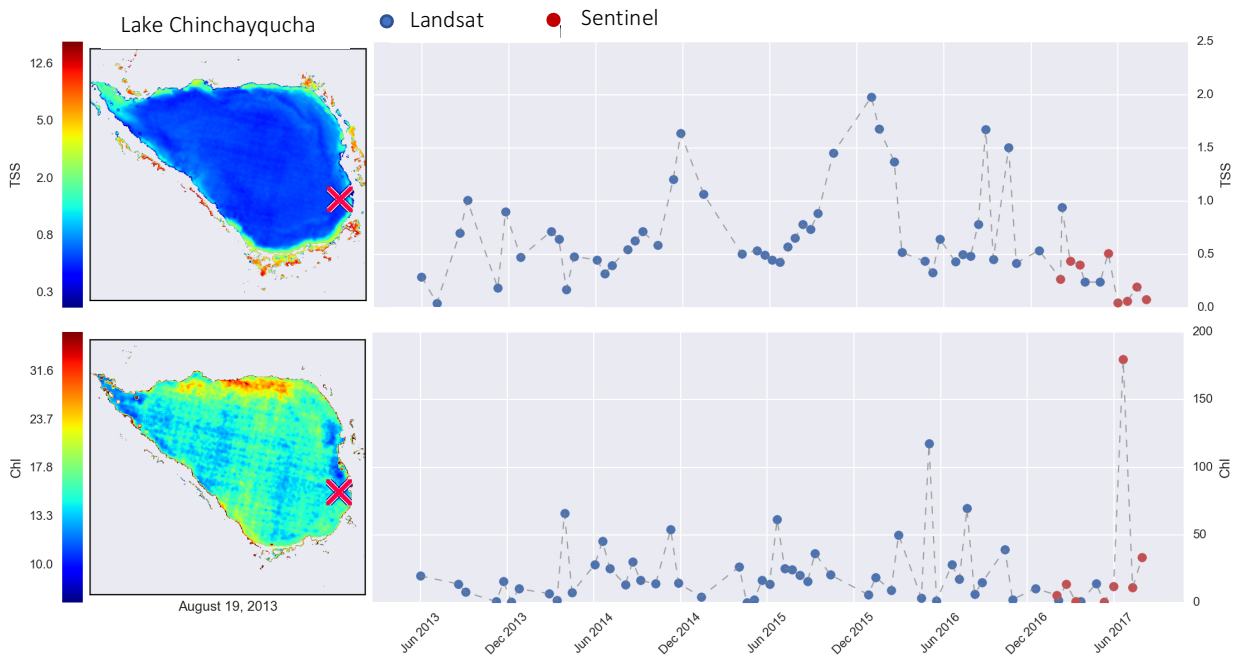

Figure 5 - Dynamics of TSS and Chl shown for the 2013-2017 period. The data points correspond to the location marked with the red cross. The temporal TSS (g/m^3) and Chl (mg/m^3) products clearly show different variations. Anomalies can fairly easily be detected using these plots (e.g., Dec 2014 and Dec 2016 show relatively significant rise in TSS and Chl concentrations are significantly high in June 2016 and June 2017.)

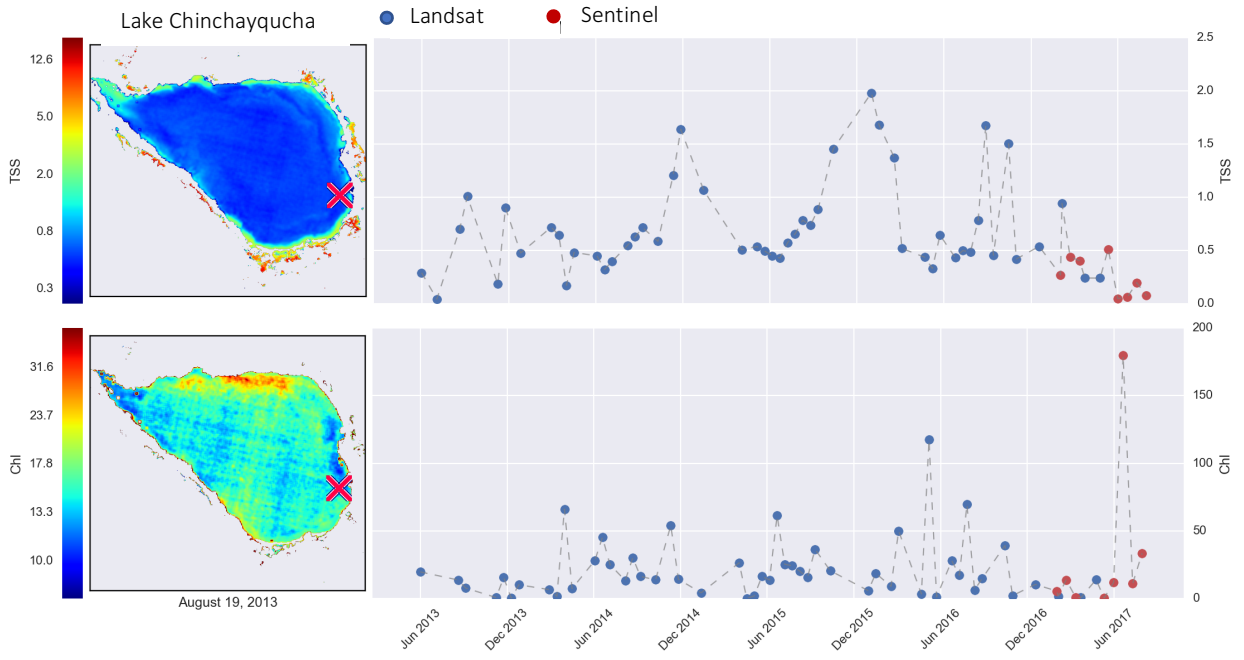

Figure 6 - Dynamics of TSS and Chl shown for the 2013-2017 period. The data points correspond to the location marked with the red cross. The temporal TSS (g/m^3) and Chl (mg/m^3) products clearly show different variations. Anomalies can fairly easily be detected using these plots (e.g., Dec 2014 and Dec 2016 show relatively significant rise in TSS and Chl concentrations are significantly high in June 2016 and June 2017.)

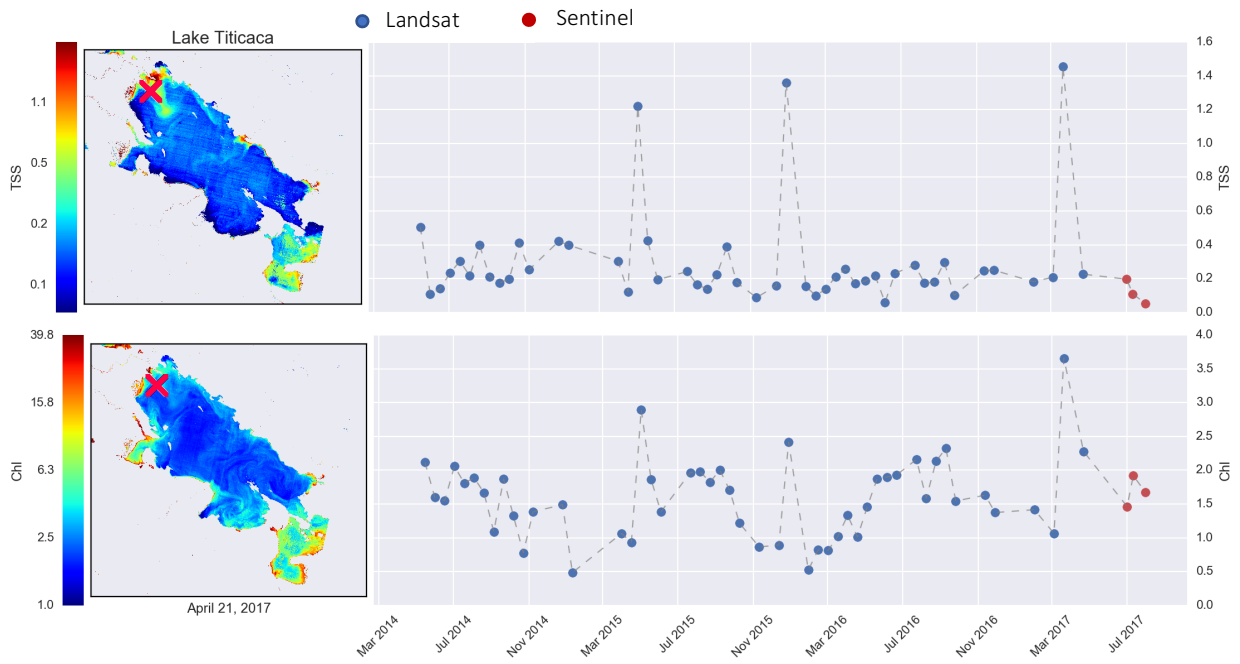

Figure 7 - Dynamics of TSS and Chl shown for the 2014-2017 period. The data points correspond to the location marked with the red cross. The temporal TSS (g/m^3) and Chl (mg/m^3) products clearly show different variations. Anomalies can fairly easily be detected using these plots. The TSS concentrations are high (relative to average) in March and November of 2015during which Chl concentration also peaks.

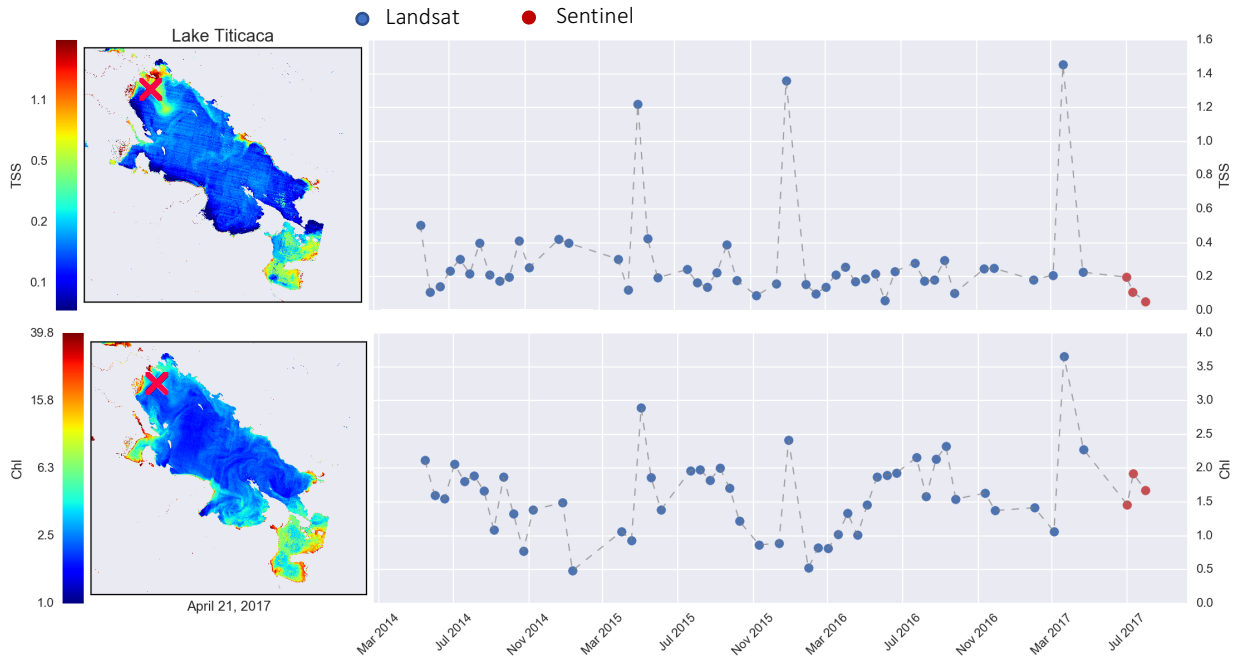

Figure 8 - Dynamics of TSS and Chl shown for the 2014-2017 period. The data points correspond to the location marked with the red cross. The temporal TSS (g/m^3) and Chl (mg/m^3) products clearly show different variations. Anomalies can fairly easily be detected using these plots. The TSS concentrations are high (relative to average) in March and November of 2015during which Chl concentration also peaks.

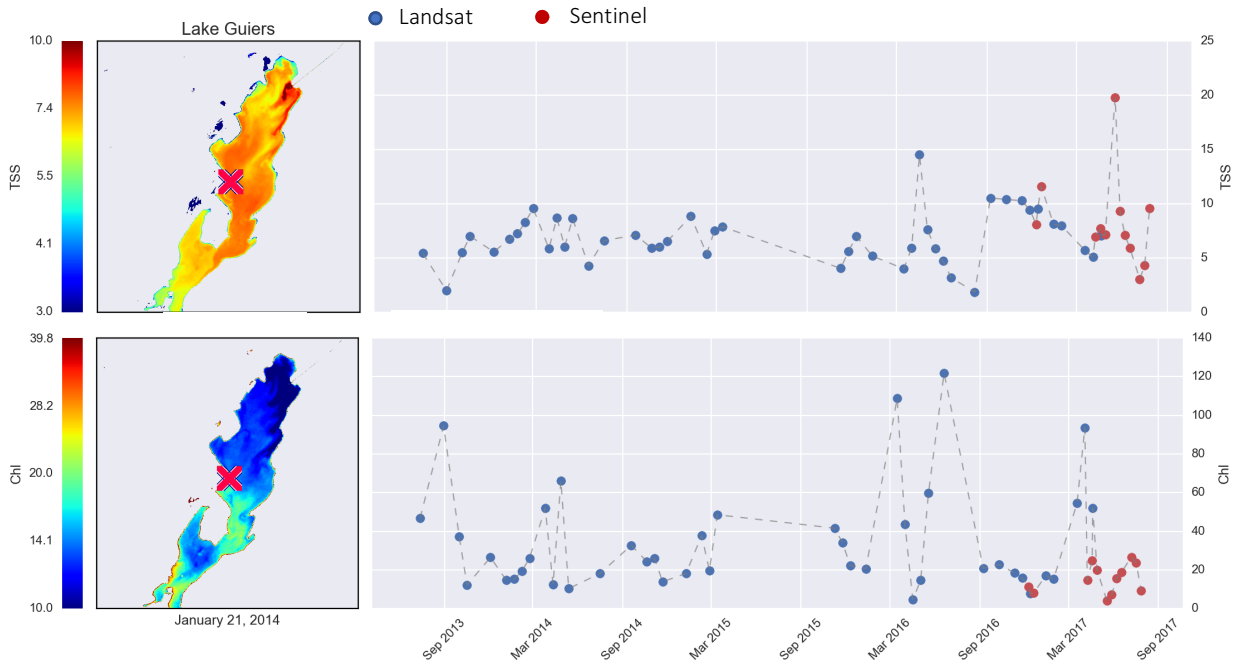

Figure 9 - Dynamics of TSS and Chl shown for the 2013-2017 period. The data points correspond to the location marked with the red cross. Anomalies in recent years can fairly easily be detected using time-series plots. The TSS concentrations are high (relative to average) in March and November of 2015during which Chl concentration also peaks. Chl concentrations indicate three major anomalies in spring of 2016 and 2017.

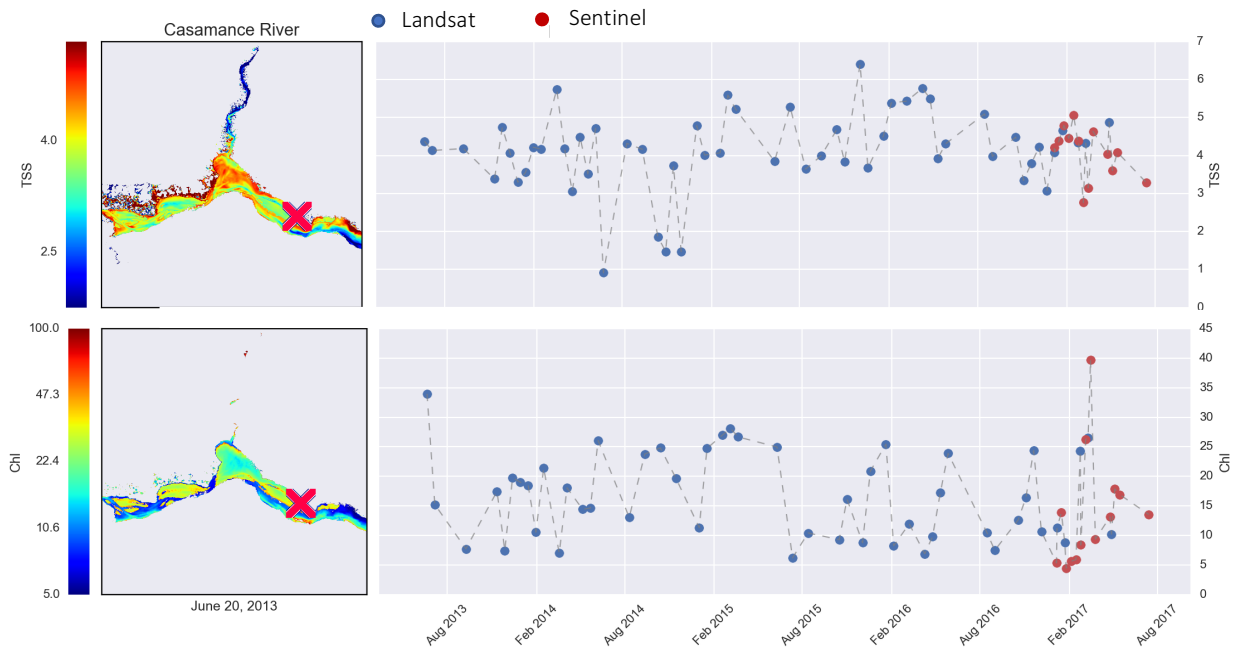

Figure 10 - Dynamics of TSS and Chl shown for the 2013-2017 period. The data points correspond to the location marked with the red cross. Anomalies in recent years can fairly easily be detected using time-series plots. The Chl concentration indicates a major peak in Feb 2017. The TSS concentrations do not show any particular peaks or trends.

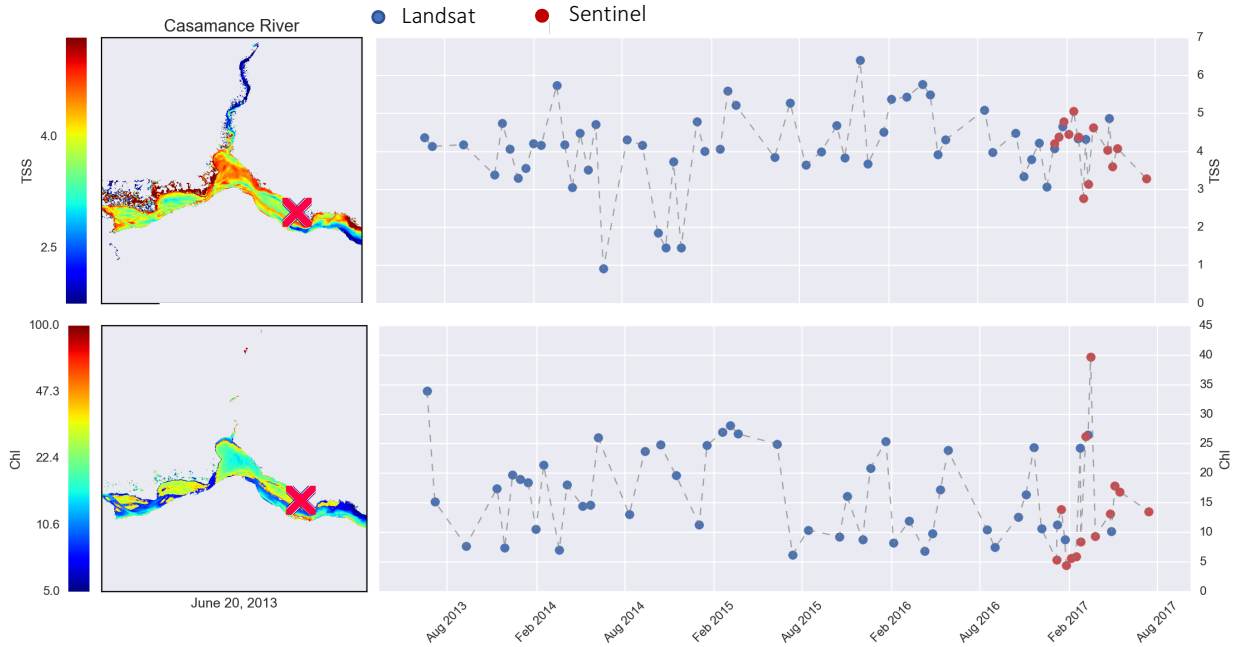

Figure 11 - Dynamics of TSS and Chl shown for the 2013-2017 period. The data points correspond to the location marked with the red cross. Anomalies in recent years can fairly easily be detected using time-series plots. The Chl concentration indicates a major peak in Feb 2017. The TSS concentrations do not show any particular peaks or trends.

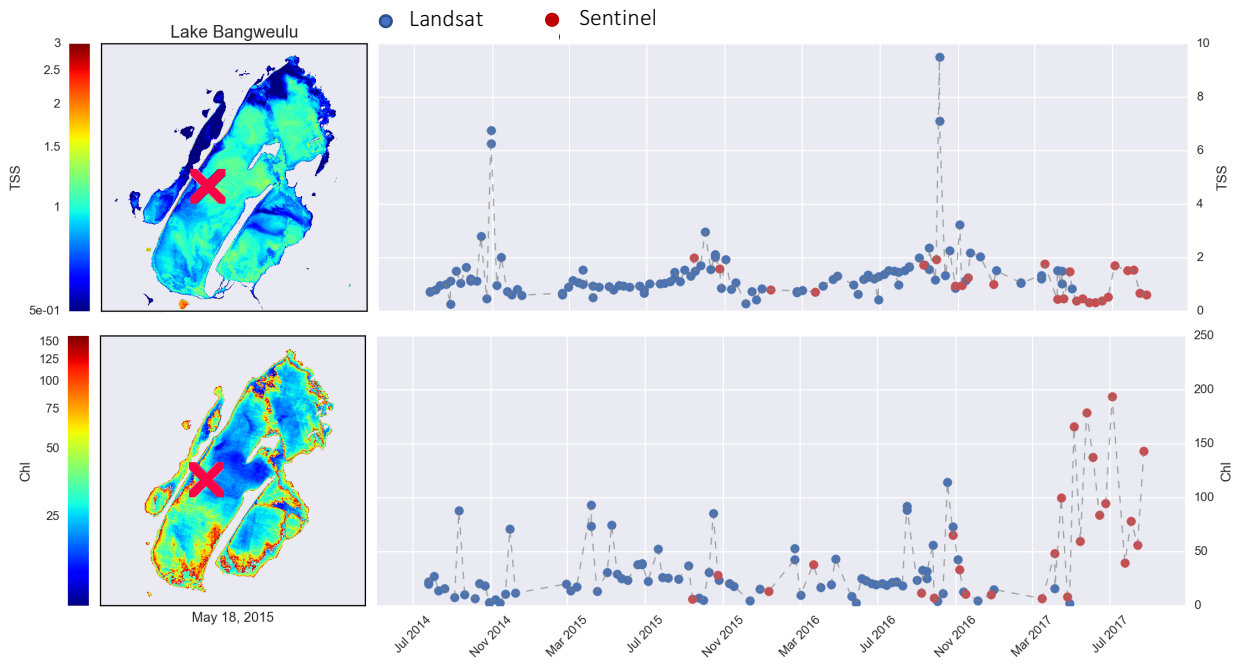

Figure 12 - Dynamics of TSS and Chl shown for the 2013-2017 period. The data points correspond to the location marked with the red cross. Anomalies in recent years can fairly easily be detected using time-series plots. Very high Chl concentrations can be observed on a regular basis. The average Chl concentration significantly increase since March 2017. Two major peaks November of 2014 and 2016 may indicate a major rainfall event.

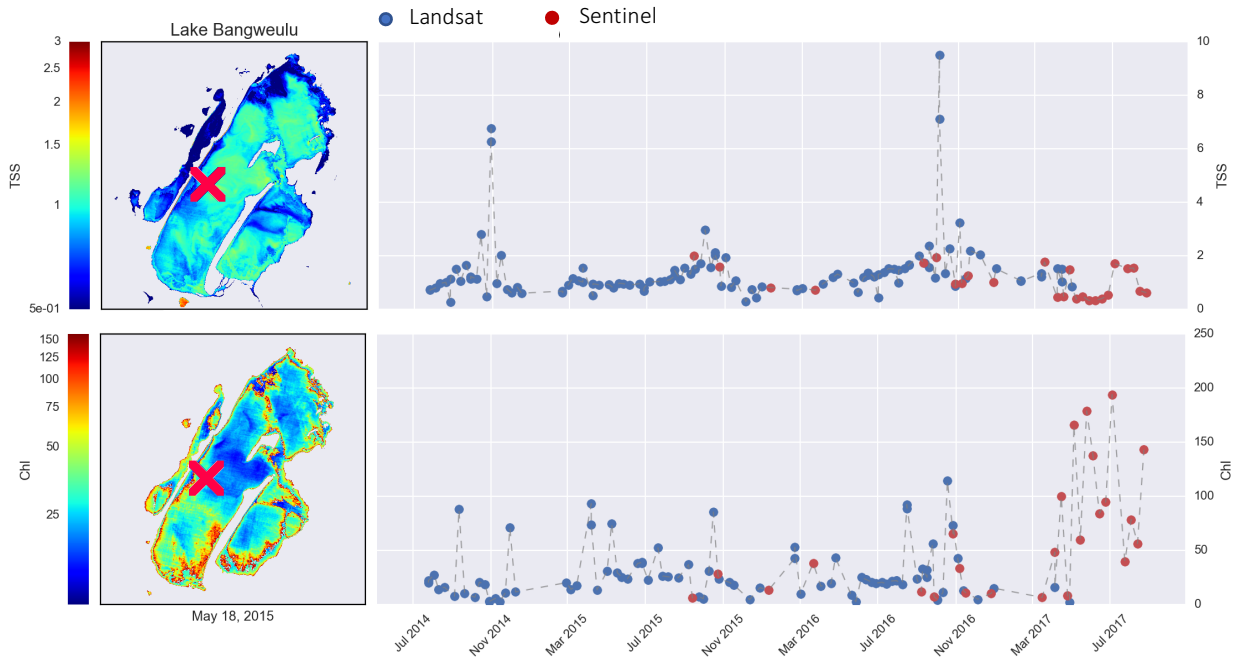

Figure 13 - Dynamics of TSS and Chl shown for the 2013-2017 period. The data points correspond to the location marked with the red cross. Anomalies in recent years can fairly easily be detected using time-series plots. Very high Chl concentrations can be observed on a regular basis. The average Chl concentration significantly increase since March 2017. Two major peaks November of 2014 and 2016 may indicate a major rainfall event.

5.4. Contributors

Nima Pahlevan, Brandon Smith, and Sandeep Chittimalli

6. Mapping and quantifying the spatial extent of coastal mangroves

6.1. Overview

Water Ecosystem(s) Measured: Vegetated wetlands (coastal mangroves only)

Sub-indicator(s) Measured: Spatial extent

Dataset(s): Landsat 8 OLI**,** Sentinel-1C**,** Shuttle Radar Topography Mission Elevation Data

Data Source(s): to be provided

Spatial Resolution: 30 m

Required Software: Google Earth Engine, QGIS (or other Geographic Information Systems Software)

Output Format(s): GeoTiff

Relevant Publications:
Lagomasino,D., Fatoyinbo, T., Lee, S.K., Feliciano, E., Trettin, C., Shapiro, A., and Mangora, M. Large-scale assessment of mangrove stand age and growth show rapid colonization in deltas. (*in preparation*)

6.2. Methodology

The data used for this analysis consisted of 30 m resolution Landsat 8 Operational Land Imager (OLI), Sentinel-1C, and Shuttle Radar Topography Mission (SRTM) elevation data. Landsat data were preprocessed which included image resampling, conversion to top of atmosphere reflectance, cloud and shadow removal and quality assessment, and image normalization. Landsat 8 OLI bands were used as inputs for the classification, as well as normalized band ratios Normalized Difference Vegetation Index (NDVI), normalized water index, normalized burn ratio, and others outlined in Green et al, 1998). Additionally, annual maximum 'VV' and 'VH' metrics from Sentinel-1C and elevation data from SRTM were also resampled and included in the classification. Areas where SRTM elevation was over 50 meters and areas where the annual maximum NDVI value were less than 0 were masked out prior to analysis to improve the classification. By doing this, areas where the elevation was too high or areas of permanent water bodies were removed, respectively. A K-means clustering algorithm was used to generate 60 land cover types using 10000 randomly samples points within the area of analysis. Automatic detection of the land cover types were then merged into mangrove and non-mangrove classes using visual interpretation of the annual 2016 Landsat composite. Google Earth imagery was used extensively as an additional reference for the 2016 classification.

A NDVI anomaly was calculated for each study region using the Landsat image archives. The reference period covered Landsat 5TM images from January 1990 through December 1999. Images were preprocessed following a similar criterion as the mangrove extent. A mean NDVI value was generated from the sum of individual pixels across all the images that were normalized by the number images

representing non-null values. The mean NDVI for the reference period (1990-2000) was then subtracted from each of the images in the observation period which ranged from January 2000 through December 2016. The anomaly value from each overlapping pixel was then summed across all the images in the collection to determine an overall cumulative anomaly. The cumulative anomaly values were also normalized for the total number of images with non-null values for individual pixels. Anomalous NDVI values were considered those which fell outside the 5th and 95th percentiles over the study region. Values greater than the 95th percentile were considered areas of forested gain, while those values less than the 5th percentile were characterized as forested areas that were lost. Gains in mangrove area from 2000 to 2016 were assumed to only occur within the 2016 extent as mapped for this study. Conversely, any loss during the 16-year period is assumed to only occur within the mangrove extent in 2000 as mapped by Giri et al, 2010. The mangrove extent maps for 2000 and 2016 were used to mask regions of losses and gains, respectively, from the NDVI anomaly.

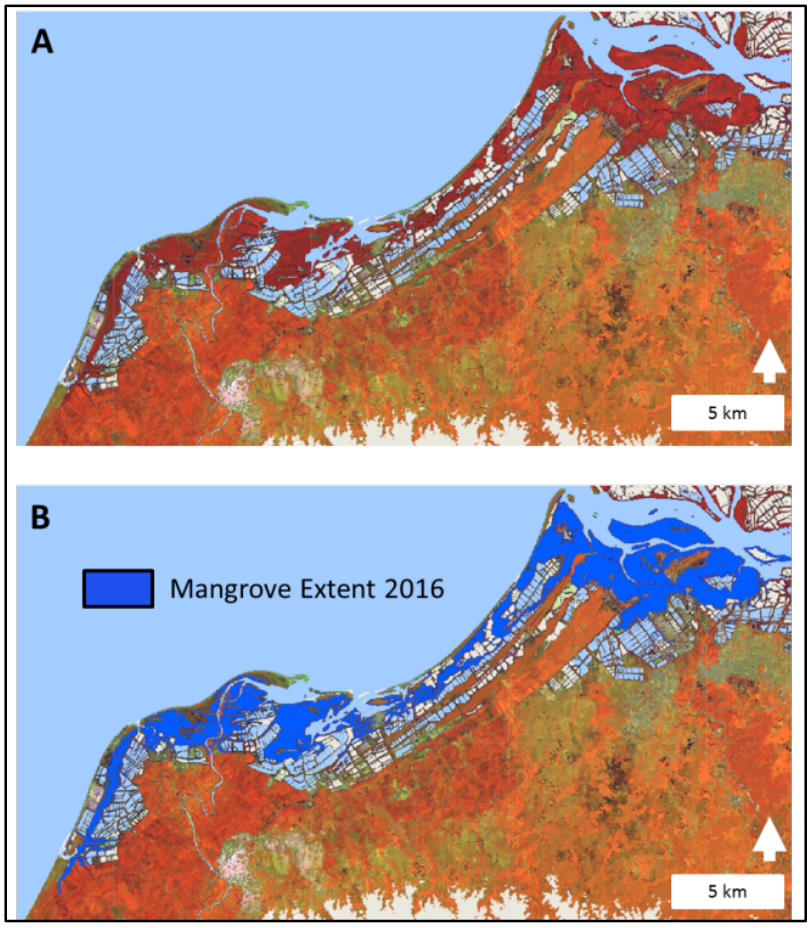

Figure 14 - A) The near-infrared, short-wave infrared, and red bands from Landsat 8 OLI were used to make this 2016 false-color composite of Northern Peru (Tumbes District). B) Mangrove wetlands in 2016 can be mapped using remote sensing, the results of which are shown in dark blue. Open water areas are shown in light blue.

6.3. Results

Table 4 – Spatial extent of coastal mangroves for three pilot countries, extracted using Landsat, Sentinel and SRTM data, as described in the above methodology.

Country	Assessment period	Spatial extent of coastal mangroves (km^2)
Senegal	2016	1902.8
Peru	2016	54.3
Jamaica	2016	86.6

Source of Administrative boundaries: The Global Administrative Unit Layers (GAUL) dataset, implemented by FAO within the CountrySTAT and Agricultural Market Information System (AMIS) projects.

6.4. Contributors

Lola Fatoyinbo, NASA Goddard Space Flight Center, Biospheric Sciences
David Lagomasino, University of Maryland, Geographical Sciences

7. Discussion

This document provides a brief description of the methodologies used for the application of specific EO datasets to meet the reporting requirements of SDG 6.6.1 in terms of open waterbody water extent, inland water quality (two optically detectable parameters) and the extent of coastal mangroves (partially meeting the requirement for the monitoring and reporting of wetlands). In addition to sharing an overview of the methodology, country-level values are extracted for select pilot countries to demonstrate the potential for the application of these methods in SDG reporting. However, these values in no way provide official country baseline values for Indicator 6.6.1, as it is the sole responsibility of individual countries to report on baseline values for this indicator as well as all other indicators relevant to the SDGs. The document serves as a proof of concept for similar future applications and provides a means for countries to replicate and adapt the methods to meet their needs. All of the EO datasets that were used are of global coverage and freely and publically available, making them a particularly attractive option for data-scarce regions. The availability of high-quality, relatively frequent satellite products together with existing algorithm/methodologies and validation using in-situ and ground based data also enables reporting on relative changes from baseline values over time in a more consistent and systematic manner.

Regarding the two products used to map and measure the extent of open waterbodies, Landsat can resolve much smaller features than MODIS, and therefore Landsat-based water products will be able to map smaller water bodies than MODIS is able to capture. On the other hand, annual maps created from MODIS data, with its daily repeat coverage, have a higher likelihood of accurately measuring surface water extent in areas with limited imagery due to cloud cover than those created from sensors with lower temporal resolution, such as the Landsat constellation, which between Landsats 7 and 8 images the globe once every 8 days. Both Landsat and MODIS water products should only be used to study waterbodies that are at minimum the length of several pixels in each dimension, which means Landsat is the most appropriate choice for smaller waterbodies, including rivers. MODIS is more appropriate for medium to large waterbodies that are either in cloudy areas or that change rapidly; medium to large water bodies that do not meet these criteria can be accurately mapped with either sensor. The difference in spatial resolution between the two products, along with the different assessment periods and methodologies used (due to the nature of MODIS versus Landsat data), accounts for the difference in reported numbers for the seven pilot countries. In most cases Landsat estimated a larger extent area for open waterbodies than did

MODIS, which is an expected outcome given that Landsat is able to capture more small water bodies and rivers.

Water quality measurements from EO data presents an exciting new opportunity for SDG reporting, and in general for many end-user communities interested in assessing the health and condition of waterbodies over time. The Landsat-Sentinel-2 satellite data, if processed via appropriate tools, enables capturing dynamics of SDG water quality indicators, including concentrations of chlorophyll-a (Chl) and total suspended solids (TSS), two of the water quality indicators required for reporting. For a more robust use of satellite data products for water quality monitoring, a close collaboration between the EO community and local/regional authorities is needed. Through a collaborative approach, EO data can help to inform ground-based monitoring programs, thus enabling a more cost-effective means for the monitoring of water quality. In the future, the NASA Goddard Space Flight Center is planning to develop a satellite-based water quality warning system. This system can be evaluated and tested for several bodies of water in various developing countries having close ties with the UN Environment partners, and contribute towards progressive monitoring of Indicators 6.3.2 and 6.6.1.

Although the wetlands mapping methodology shared in this document does not cover all wetlands, the mangrove extent data can be used to generate country and district-wide extent estimates, which can be applicable for many countries. The data represent an average extent for the year and does not capture the highly dynamic nature of mangroves. The supplemental land cover change dataset provides information on the long-term trends in mangrove change. Trends of excessive gain or excessive loss can be useful in determining key locations for future sustainable development projects, such as those related to coastal resilience, in addition to helping countries meet their SDG reporting requirements for Indicator 6.6.1.